Appl Biochem Biotechnol (2017) 182:609–623
DOI 10.1007/s12010-016-2348-5

Size-Selective Harvesting of Extracellular Vesicles for Strategic Analyses Towards Tumor Diagnoses

Chihiro Manri[1] · **Takahide Yokoi**[1] · **Hirokazu Nishida**[1]

Received: 22 July 2016 / Accepted: 24 November 2016 /
Published online: 5 December 2016

Abstract Extracellular vesicles (EV), typified by exosomes or microvesicles, are expected to be effective diagnostic markers for cancers. The sizes of the vesicles range from 20 to 1000 nm, but the size-dependent variations of the contents of EVs are still poorly understood. We succeeded in the size-selective harvesting of the vesicles by utilizing the molecular weight-dependent characteristics of a variety of polyethylene glycols (PEG) as precipitating reagents and analyzed the antigens displayed on the surfaces of the vesicles and the miRNAs included in the vesicles from each size group. As a result, the relatively larger (<100 nm) particles precipitated by PEG5k clearly exhibited the greatest amount of epithelial cell adhesion molecule (EpCAM), from both breast cancer (MCF-7) and colon cancer (HCT116) cells, and a larger quantity of microRNA (miRNA) specific to breast cancer cells (miRNA155 for MCF-7) seemed to be contained in the PEG-precipitated particles. The results demonstrated that the quantities of both the tumor-specific miRNA and protein were similarly distributed among the several classes of the size-sorted EVs and that the size-selective harvesting of EVs may be informative for strategic analyses towards the diagnoses of cancers.

Keywords Extracellular vesicles · Exosome · Microvesicle · Tumor marker diagnosis · Polyethylene glycol

✉ Hirokazu Nishida
h.nishida2@kurenai.waseda.jp; nishidahrk@nedo.go.jp

Chihiro Manri
chihiro.manri.kf@hitachi.com

Takahide Yokoi
takahide.yokoi.gz@hitachi.com

[1] Center for Technology Innovation—Healthcare, Hitachi Ltd., Research & Development Group, 1-280 Higashi-koigakubo, Kokubunji, Tokyo 185-8601, Japan

Introduction

Living cells release different types of membrane vesicles from endosomal and plasma membrane origins, called exosomes and microvesicles, respectively, into a variety of body fluids, such as plasma, lymph, ascites, amniotic fluid, saliva, etc. (reviewed in [1, 2]). These extracellular vesicles (EVs) represent an important mode of intercellular communication, by serving as vehicles for transferring membrane and cytosolic proteins, lipids, and RNA between cells.

The term exosome was initially the nomenclature for vesicles ranging from 40 to 1000 nm that are released from various cultured cells [3]. Subsequently, the exosome was defined as the 40–140 nm vesicles released as a result of multivesicular endosome (MVE) fusion with the plasma membrane. Specifically, microvesicles are directly released to the extracellular space by the outward budding of the plasma membrane, whereas exosomes are formed through the invagination of the plasma membrane into endosomes, followed by inward vesiculation, and then, the vesicle is subsequently released into the extracellular space [2, 4, 5].

MicroRNAs (miRNAs) are reportedly present in exosome preparations [6], suggesting that these vesicles may function as a vehicle for intercellular miRNA transfer and as a mode of intercellular communication [7, 8]. The miRNAs are short noncoding RNA molecules with an average length of 22 nucleotides [9]. They are transcribed as RNA hairpins and processed into mature miRNAs that bind to complementary messenger RNAs, to alter gene expression [10]. Studies on the delivery of purified exosomes to recipient cells have reported the transfer of miRNAs in experimental frameworks [11, 12], and the utilization of exosomes as compact RNA delivery vehicles is now being studied as a potent therapeutic method [13, 14].

Methods for the isolation of EVs are still being developed. At present, EVs are precipitated from the supernatants of cultured cells grown in EV-depleted fetal calf serum by ultracentrifugation. EVs are effectively isolated from nonmembranous particles, such as protein aggregates, by their low buoyant density [15, 16]. The separation of different size classes of EVs can be roughly achieved by the differences in the sedimentation coefficients of each class of EVs. However, accurate size separation is difficult to reproduce, since the differences in the sedimentation coefficients of EVs are not necessarily sufficient for separation by centrifugation. Another method for the efficient isolation of EVs involves immunoadsorption, by targeting a protein of interest [17].

Since exosomes and microvesicles have recently attracted keen attention as biomarkers for diseases, kits that facilitate their isolation are now commercially available.

Polyethylene glycols (PEGs) have been utilized as precipitating reagents for several biological macromolecules, such as proteins and DNA, and even for the isolation of viral and EV particles from cultivation medium [18–20]. The molecular weight-dependent characteristics of PEGs as precipitants in protein crystallization are important in structural biology [21]. Generally, the high-molecular-weight PEGs more potently precipitate the macromolecules dissolved in solution, as compared to the same weight/volume concentration of the low-molecular-weight PEGs [22].

Here, we report the size-selective separation of EV particles, without the separation of the EVs into exosome and microvesicle fractions, by using different molecular weight polyethylene glycols as precipitants. We performed the size-dependent characterization of EVs by enzyme-linked immunosorbent assay (ELISA), targeting the exosome-specific markers (CD9, CD63) and the epithelial cell adhesion molecule (EpCAM) of EVs in culture media from breast cancer (MCF-7) and colon cancer (HCT116) cells. We also performed quantitative

real-time reverse transcription-PCR, focused on the breast cancer-originated miRNAs for MCF-7. The search for the cancer-originated marker of MCF-7 is still in progress [23].

Our one-step precipitation method utilizing different molecular weight PEGs is useful for the size selection of EVs, which may facilitate strategic analyses towards the diagnoses of cancers.

Materials and Methods

Cell Culture

The breast cancer cell line (MCF-7) and the colon cancer cell line (HCT116) were purchased from American Type Culture Collection (Manassas, VA, USA) and DS Pharma Biomedical (Osaka, Japan), respectively. Cells were cultured according to the supplier's instructions, with slight modifications. Both cell lines were subcultured every 7 days.

Size-Selective Isolation of Particles from the Culture Medium

We prepared the precipitating reagents for the size-selective isolation of particles using different molecular weight polyethylene glycols: PEG5k, PEG8k, PEG10k, and PEG20k, purchased from Sigma-Aldrich (St. Louis, MO, USA). The PEGs were dissolved (50% *w*/*v*) in PBS with 0.5 M NaCl (PBS-HS) and then utilized as the precipitating reagents.

EVs were isolated from the culture supernatants of the HCT116 and MCF-7 cell lines. A 50 mL portion of the supernatant was collected and centrifuged at 3000×*g* for 15 min at 4 °C, in order to remove debris. The supernatant was divided equally (10 mL each) into five tubes, and each was mixed with 2 mL of the precipitating reagents or the commercially available ExoQuick TC solution, from System Biosciences (Mountain View, CA, USA). The tubes were centrifuged at 10,000×*g* for 15 min at 4 °C, and the precipitates thus obtained were used in the subsequent analyses.

Scanning Electron Microscopic Analyses of EVs

For scanning electron microscopy (SU8020, Hitachi High-Technologies, Japan), the PBS-suspended exosomes were fixed on the (3-aminopropyl)triethoxysilane (Sigma-Aldrich GmbH)-treated Si substrate for 24 h. After washing with PBS for 5 min, the electrostatically immobilized exosomes were soaked in 1% OsO_4 in PBS and were dehydrated with an ascending sequence of ethanol percentages (40, 60, 80, 96–98%). After the ethanol was evaporated, the samples were left to dry at room temperature for 24 h on the Si substrate and then analyzed by SEM after gold–palladium sputtering.

Measurement of Particle Size Distributions by the Dynamic Light Scattering Method

The obtained precipitates were suspended in 200 μL of PBS-HS, and the particle size distributions of the suspensions were measured by dynamic light scattering, using an LB-550 Dynamic Light Scattering Nano-Particle Size Analyzer (HORIBA; Kyoto, Japan). We employed the refraction index of the particle as 1.600 for a typical organic sample and that of

the disperse media as 1.333 for water. The scattering data were measured 50 times and then averaged.

We analyzed the scanning data, determined the average and standard deviation values of each precipitation sample, and calculated the p values between all combinations of the precipitated samples. The one-tailed t test for quantitative variables was performed using Statplus (AnalystSoft, Walnut, CA). The presented p values were determined by the two-tailed test.

ELISA Analyses of Size-Selectively Isolated EVs

To standardize the quantities of the exosomes included in the precipitates, we performed an ELISA to detect CD63 and CD9, which are abundantly produced in exosomes. To evaluate the tumor cell-specific exosomes, we also performed an ELISA targeting the tumor cell marker EpCAM. The precipitates obtained with the PEG solutions or ExoQuick TC were dissolved in 400 μL of exosome binding buffer from the ExoELISA kit (System Biosciences) and incubated at 37 °C for 20 min. Aliquots (50 μL each) of the solution were placed into the wells of a 96-well ExoELISA plate and incubated overnight at 37 °C. Subsequent ELISA reactions were performed according to the manufacturer's instructions, and the absorbance data were measured using a TECAN Infinite F500 microplate reader (Männedorf, Switzerland).

Cytokeratin 19 (CK19) is potentially useful for detecting tumors in breast cancer patients [24]. To evaluate the expression level of the breast cancer-specific marker CK19 within the size-separated precipitates isolated from the supernatants of the MCF-7 cell line, we performed ELISA experiments as described above.

Quantitative Real-Time Reverse Transcription-PCR Focused on Detecting Breast Cancer-Originated miRNAs

Total RNA was isolated from the EVs, using a Total Exosome RNA and Protein Isolation Kit (Thermo Fisher Scientific; Waltham, MA, USA) according to the manufacturer's instructions. The reverse transcription reactions of the obtained RNA were performed using a TaqMan Micro RNA Reverse Transcription Kit (Thermo Fisher Scientific), with primers selected from the TaqMan Micro RNA Assays (Thermo Fisher Scientific). The polymerase chain reaction was performed using TaqMan Micro RNA Assays (Thermo Fisher Scientific) and analyzed by a 7900HT Fast Real-Time PCR System (Thermo Fisher Scientific). All reactions were done in triplicate. The concentrations of the miRNAs were calculated based on their C_t values normalized to those of miRNA16, which was spiked at 1 nM in each aliquot of the reaction mixture [25, 26].

Results

Size-Selective Isolation of Particles from Culture Media

The precipitations by the different molecular weight PEGs, PEG5k, PEG8k, PEG10k, and PEG20k revealed that the lower molecular weight PEGs precipitated smaller amounts of particles, consistent with the ELISA experiment targeting the exosome-originating CDs

described in the next section. The wet weights of the obtained precipitates from the fixed solution volume (10 mL) were 4.1 ± 1.4 mg (PEG5k), 9.1 ± 3.3 mg (PEG8k), 15.9 ± 7.1 mg (PEG10k), and 22.0 ± 8.6 mg (PEG20k) for HCT116 and 3.7 ± 1.1 mg (PEG5k), 5.1 ± 2.4 mg (PEG8k), 12.6 ± 5.5 mg (PEG10k), and 15.0 ± 6.5 mg (PEG20k) for MCF-7. The mean values and the deviations were calculated from three independent precipitation trials. The wet weights were the difference in the weights before and after the removal of the precipitates in 10-mL plastic tubes.

The dynamic light scattering analysis indicated homogeneous populations with a single mean size, except for the PEG5k precipitate. In the case of PEG5k, we separated two peaks with 780 nm as a border and calculated the average and the standard deviation for each peak. The size distributions of the particles were different between the precipitates obtained with the different molecular weight PEGs (Fig. 1a–d). The PEG5k-precipitated HCT116 suspension showed the largest median values of 144–190 nm, whereas the PEG20k-precipitated suspension exhibited median values of 53–62 nm. The PEG8k and PEG10k-precipitated suspensions of HCT116 displayed medium-sized values, 87–123 nm (PEG8k) and 68–94 nm (PEG10k). In the case of MCF-7, the PEG5k-precipitated suspension showed the largest median values of 115–131 nm, whereas the PEG20k-precipitated suspension exhibited median values of 43–49 nm. The PEG8k and PEG10k-precipitated MCF-7 suspensions displayed medium-sized values, 80–90 nm (PEG8k) and 54–76 nm (PEG10k). The ExoQuick-precipitated particles exhibited the same characteristics as the PEG20k-precipitated particles, 51–76 nm for HCT116 and 36–61 nm for MCF-7. Using the representative distribution bar charts (from the distribution samples in the left panel in Fig. 1a for HCT116 and the left panel in Fig. 1b for MCF-7), we determined the p values between all combinations of precipitated samples. Judging from the p values for HCT116, PEG20k and ExoQuick showed the same tendency, whereas the other combinations exhibited low p values ($p < 0.05$), suggesting that the different molecular weight PEGs are useful for sorting the particle sizes. In the case of MCF-7, the particle size distributions precipitated by PEG8k and PEG10k resembled each other ($p = 0.1731$).

SEM Analyses of EVs

The electrostatic immobilization of EVs with a self-assembled monolayer of (3-aminopropyl)triethoxysilane on the Si substrate was inefficient, and the EV particles were very sparsely fixed on the substrate. Representative particles observed from each precipitation experiment are shown in Fig. 1e. The sizes of the observed particles were consistent with the results from the dynamic light scattering experiments described above.

ELISA Experiments Targeting the Exosome-Originating CDs

To standardize the quantities of exosomes included in the precipitations, we performed ELISA experiments targeting CD9 and CD63 (Fig. 2a, b). The relative amounts of CDs in the precipitates showed a similar trend between CD9 and CD63, from both HCT116 and MCF-7. The PEG5k-precipitated and PEG8k-precipitated samples contained relatively low quantities of the proteins in the precipitates. In contrast, the PEG20k-precipitated and ExoQuick-precipitated samples contained the largest amounts of the proteins in the precipitates, consistent with their visually judged quantities.

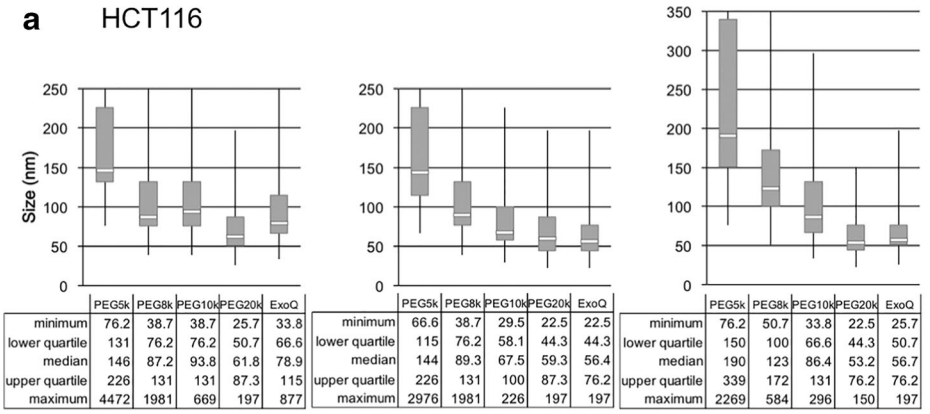

Fig. 1 Boxplot representations of the particle size distributions obtained using different PEGs (PEG5k, PEG8k, PEG10k, and PEG20k) and ExoQuick, and SEM images of the particles obtained from each precipitation experiment. **a** Box plots of the precipitates obtained for HCT116 from three independent experiments. The median value of each precipitate is highlighted by a *white line*. The *gray boxes* indicate the ranges including 50% of the precipitated particles. The minimum, lower quartile, median, upper quartile, and maximum values are indicated in the tables below the charts. **b** Box plots for MCF-7. **c** The detailed size distributions of the representative box plot (the *left panel* in **a**) and the average and standard deviation values for HCT116 (*top*). The list of *p* values calculated for all combinations of PEGs (PEG5k, PEG8k, PEG10k, and PEG20k) and ExoQuick for HCT116, in which significantly low *p* values ($p < 0.05$) are highlighted in *bold* (*bottom*). **d** The detailed size distributions of the representative box plot (the *left panel* in **b**) and the average and standard deviation values for MCF-7 (*top*). The list of *p* values calculated for all combinations for MCF-7, in which significantly low *p* values ($p < 0.05$) are highlighted in *bold* (*bottom*). **e** SEM images of particles immobilized on the self-assembled monolayer of (3-aminopropyl)triethoxysilane on the Si substrate, obtained using PEG5k (*upper left*), PEG8k (*upper right*), PEG10k (*bottom left*), and ExoQuick (*bottom right*)

ELISA Experiments Targeting EpCAM

To examine the precipitates for the presence of EpCAM, a diagnostic marker for various cancers, we performed ELISA experiments targeting EpCAM.

In contrast to the aforementioned experiments, the EpCAM-targeted ELISA experiment clearly revealed that the PEG5k-precipitated largest-sized particle samples from both HCT116 and MCF-7 included the highest amount of EpCAM, despite the smallest amounts of the precipitates and the low levels of CD9 and CD63 (Fig. 2c). The PEG20k-precipitated and ExoQuick-precipitated small-sized particle samples included the largest amounts of the precipitates and CDs but relatively smaller amounts of EpCAM in the cases of both HCT116 and MCF-7.

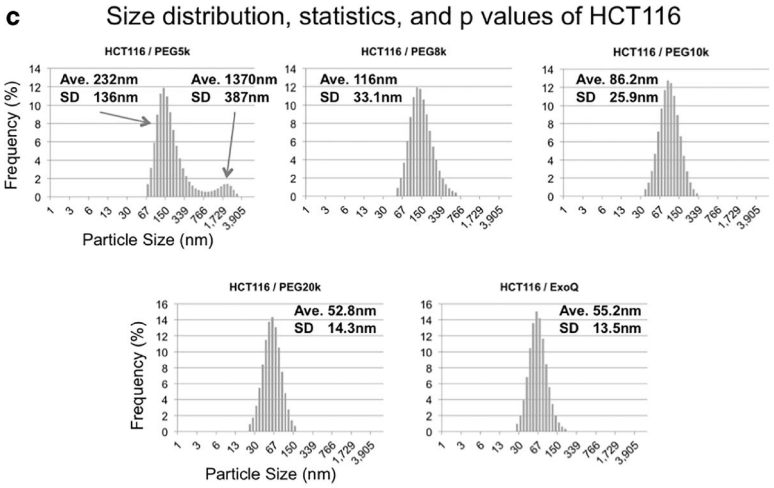

p values					
HCT116	**PEG5k**	**PEG8k**	**PEG10k**	**PEG20k**	**ExoQ**
PEG5k	-	**0.00019**	**1.90E-06**	**7.25E-07**	**5.37E-07**
PEG8k	-	-	**0.0135**	**0.0023**	**0.0013**
PEG10k	-	-	-	**0.0249**	**0.0036**
PEG20k	-	-	-	-	0.4664

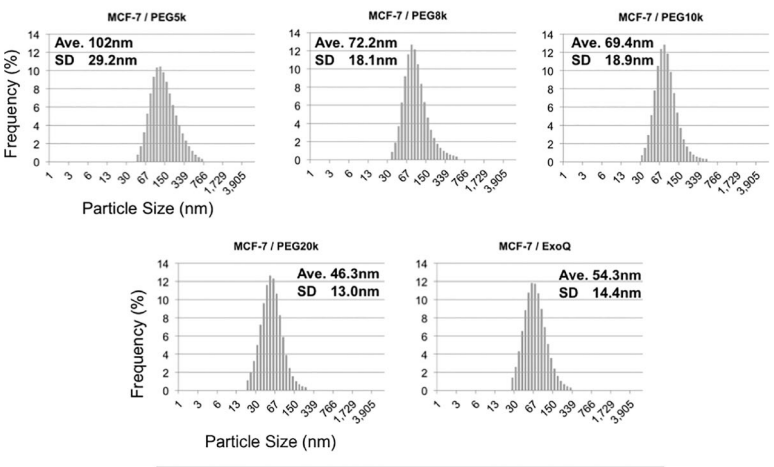

p values					
HCT116	**PEG5k**	**PEG8k**	**PEG10k**	**PEG20k**	**ExoQ**
PEG5k	-	**2.71E-05**	**7.39E-08**	**2.30E-17**	**1.59E-12**
PEG8k	-	-	0.1731	**5.61E-09**	**0.00025**
PEG10k	-	-	-	**3.64E-07**	**0.0117**
PEG20k	-	-	-	-	**0.0023**

Fig. 1 (continued)

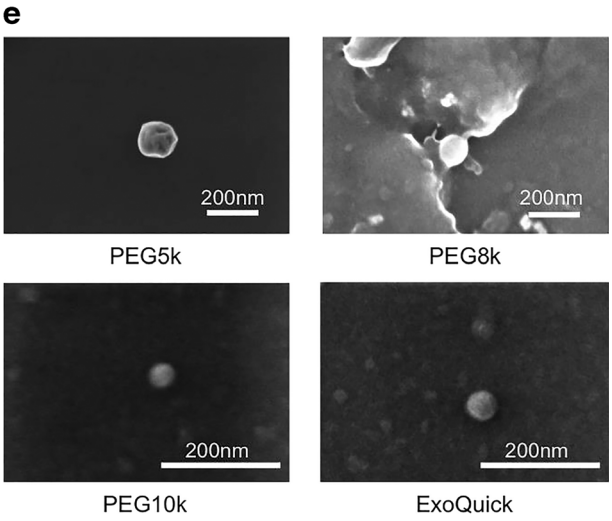

Fig. 1 (continued)

Quantitative Real-Time Reverse Transcription-PCR Technique

To confirm that the tumor-specific miRNAs actually exist in the isolated particles, we performed a quantitative real-time reverse transcription-PCR experiment focusing on miRNA21 and miRNA155, which are specific to breast cancer exosomes [25, 26]. The obtained C_t values for the size-separated precipitation classes from MCF-7 are summarized in bar charts (Fig. 3a–c left), flanked by a table of p values for all possible pairs of C_t values (Fig. 3a–c right). The miRNA16-normalized relative amounts of miRNA21 and miRNA155 (delta-delta C_t method) for each precipitation class are listed in Table 1.

The normalized relative amounts of miRNA including EVs ranged from 0.4 to 0.8 for miRNA21 and from 0.9 to 1.9 for miRNA155. The amounts of miRNA155 seemed to be differently distributed in each precipitation class. In contrast, miRNA21 was distributed more evenly over all precipitation classes, consistent with the fact that the precipitation quantity increased according to the molecular weight of the PEG.

ELISA Analyses of the Breast Cancer-Specific Marker CK19

As in the ELISA experiments described above, the CK19-targeted ELISA experiment revealed that the PEG5k-precipitated, largest-sized particle samples from the breast cancer cell line MCF-7 included the highest amount of CK19, among the PEG-precipitated samples, although it had the smallest amount of the precipitate (Fig. 4). However, in contrast to the ELISA experiment using EpCAM as an antigen (Fig. 2c), the PEG20k and ExoQuick-precipitated samples also contained comparable amounts of CK19. Although the actual reason for this phenomenon is unclear, the results clearly showed that the PEG5k-precipitated, largest-sized particle samples from the breast cancer MCF-7 cells contained abundant amounts of both EpCAM and CK19, suggesting that the PEG5k precipitation might be efficient for the harvesting of EVs specific to breast cancer cells.

a CD9

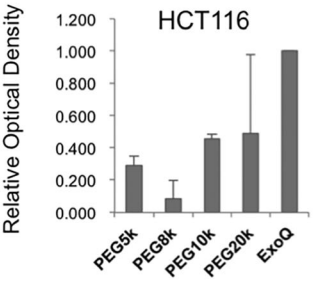

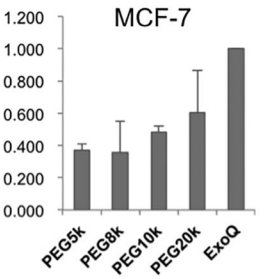

	p values				
HCT116	**PEG5k**	**PEG8k**	**PEG10k**	**PEG20k**	**ExoQ**
PEG5k	-	0.1152	0.0744	0.6369	**0.0358**
PEG8k	-	-	0.0970	0.3773	0.0537
PEG10k	-	-	-	0.9405	**0.0239**
PEG20k	-	-	-	-	0.3784

	p values				
MCF-7	**PEG5k**	**PEG8k**	**PEG10k**	**PEG20k**	**ExoQ**
PEG5k	-	0.9457	0.2848	0.4659	**0.0276**
PEG8k	-	-	0.4552	0.1148	0.1344
PEG10k	-	-	-	0.5804	**0.0334**
PEG20k	-	-	-	-	0.2767

b CD63

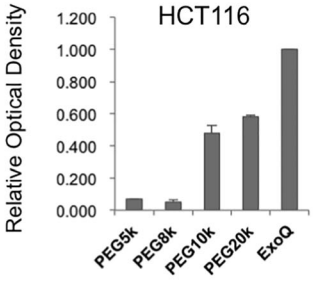

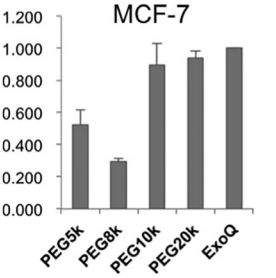

	p values				
HCT116	**PEG5k**	**PEG8k**	**PEG10k**	**PEG20k**	**ExoQ**
PEG5k	-	0.3066	0.0514	**0.0065**	**5.324 E-05**
PEG8k	-	-	**0.0376**	**0.0160**	**0.0053**
PEG10k	-	-	-	0.2331	**0.0404**
PEG20k	-	-	-	-	**0.0080**

	p values				
MCF-7	**PEG5k**	**PEG8k**	**PEG10k**	**PEG20k**	**ExoQ**
PEG5k	-	0.2139	0.0558	0.0528	0.0865
PEG8k	-	-	0.1182	**0.0449**	**0.0132**
PEG10k	-	-	-	0.6285	0.4714
PEG20k	-	-	-	-	0.2903

Fig. 2 Bar chart representations of the ELISA experiments ($n = 3$). The heights of the bars are the optical densities normalized to the intensities from the ExoQuick-precipitated samples. **a** Precipitations from HCT116 and MCF-7, using CD9 as an antigen (*top*). The list of p values calculated for all combinations of PEGs (PEG5k, PEG8k, PEG10k, and PEG20k) and ExoQuick for CD9, in which significantly low p values ($p < 0.05$) are highlighted in *bold* (*bottom*). **b** Results using CD63 as an antigen (*top*). The list of p values for CD63, in which significantly low p values ($p < 0.05$) are highlighted in *bold* (*bottom*). **c** ELISA results using the tumor-specific antigen EpCAM (*top*). The list of p values for EpCAM (*bottom*)

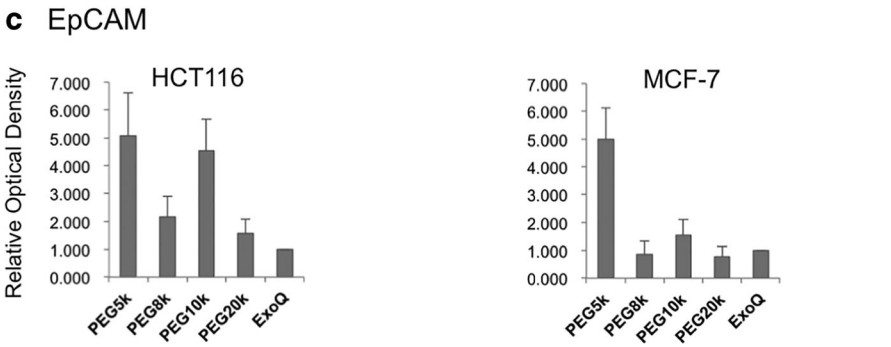

p values

HCT116	PEG5k	PEG8k	PEG10k	PEG20k	ExoQ
PEG5k	-	0.1275	0.3337	0.1313	0.1687
PEG8k	-	-	0.0760	0.1492	0.2647
PEG10k	-	-	-	0.0910	0.1414
PEG20k	-	-	-	-	0.3703

p values

MCF-7	PEG5k	PEG8k	PEG10k	PEG20k	ExoQ
PEG5k	-	0.0756	0.0749	0.0854	0.1287
PEG8k	-	-	0.0793	0.4443	0.7540
PEG10k	-	-	-	0.1331	0.4201
PEG20k	-	-	-	-	0.5340

Fig. 2 (continued)

Consistently, the CK19-targeted ELISA experiment using the ExoQuick-precipitated sample from HCT116 (H_ExoQ) contained a much lower amount of CK19, indicating that the experiments were properly performed.

Discussion

The size-selective precipitation of particles released into the culture medium was achieved by the use of different molecular weight PEGs: PEG5k, PEG8k, PEG10k, and PEG20k, suspended in high-salt-concentration (0.5 M NaCl) PBS. The resulting precipitates might include several types of EVs, such as exosomes and microvesicles, and some protein aggregates. A schematic view of the size distributions and the precipitation ranges obtained using each precipitant, plotted against the estimated quantities of the precipitates, is provided in Fig. 5.

First, we evaluated the quantities of exosomes included in each PEG-precipitated particle class by an ELISA method, targeting the CD9 and CD63 proteins, which are abundantly produced in exosomes. The results indicated that the exosome contents in the precipitates increased in accordance with the molecular weight of PEG, consistent with the quantities of the precipitates, which were also proportional to the molecular weight of PEG (Fig. 1a, b). In contrast, the mean size of the exosomes included in the precipitates decreased in accordance with the increase in the molecular weight of PEG (Fig. 5).

The particles containing EpCAM were most abundantly found in the PEG5k-precipitated largest-sized particle sample, indicating that the tumor-specific EVs were most effectively detected in the largest-sized class, in spite of the minimum quantity of the precipitate and the

a miR16

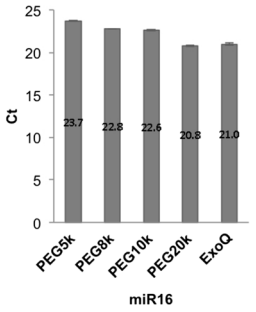

p values					
miR16	**PEG5k**	**PEG8k**	**PEG10k**	**PEG20k**	**ExoQ**
PEG5k	-	**0.00066**	**0.00386**	**0.00013**	**0.00134**
PEG8k	-	-	0.18078	**0.00040**	**0.00193**
PEG10k	-	-	-	**0.00040**	**0.00161**
PEG20k	-	-	-	-	0.15709

b miR21

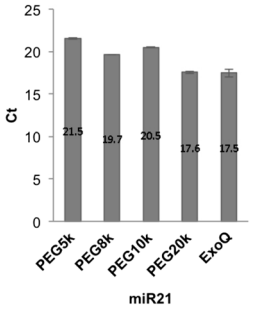

p values					
miR21	**PEG5k**	**PEG8k**	**PEG10k**	**PEG20k**	**ExoQ**
PEG5k	-	**0.00069**	**0.00030**	**0.00068**	**0.00415**
PEG8k	-	-	**0.00155**	**0.00174**	**0.01371**
PEG10k	-	-	-	**0.00118**	**0.00688**
PEG20k	-	-	-	-	0.80867

c miR155

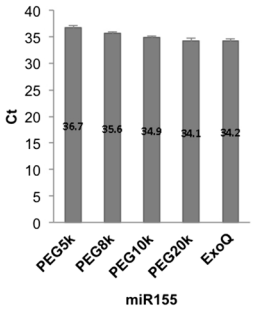

p values					
miR21	**PEG5k**	**PEG8k**	**PEG10k**	**PEG20k**	**ExoQ**
PEG5k	-	**0.01002**	**0.00090**	**0.02041**	**0.00402**
PEG8k	-	-	**0.00893**	**0.03122**	**0.03045**
PEG10k	-	-	-	0.14466	0.06320
PEG20k	-	-	-	-	0.88764

Fig. 3 Bar chart representations of the C_t values of each precipitation class from MCF-7 cells (*left*) and the list of *p* values calculated for all combinations of PEGs (PEG5k, PEG8k, PEG10k, and PEG20k) and ExoQuick (*right*), for **a** miRNA16 (control), **b** miRNA21, and **c** miRNA155, in which significantly low *p* values ($p < 0.05$) are highlighted in *bold*

minimum expression of the exosome-specific CDs (Fig. 2c). The reason why EpCAM was most abundantly found in the largest-sized class might be that the large exosomes in this precipitation class exclusively displayed EpCAM and/or that the nonexosome EVs such as microvesicles, with small amounts of CD9 or CD63, expressed large amounts of EpCAM. Indeed, the microvesicles bud directly from the plasma membrane and thus exactly reflect the membrane protein contents of the tumor cells from which they originate.

EpCAM is often utilized as an antigen for the efficient collection of cancer-derived exosomes [27]. The size selection of EVs combined with the EpCAM-targeted collection

Table 1 Standardized relative amounts of miRNA21 and miRNA155 from each MCF-7 precipitation class

	PEG5k	PEG8k	PEG10k	PEG20k	ExoQuick
miRNA21	0.40 ± 0.05	0.75 ± 0.50	0.40 ± 0.05	0.80 ± 0.10	1.0 ± 0.30
miRNA155	1.2 ± 0.30	1.3 ± 0.25	1.9 ± 0.30	0.90 ± 0.35	1.0 ± 0.25

may be an efficient method for the diagnosis of cancer-derived EVs. Especially, the harvesting of the large EVs, using PEG5k as a precipitant, may be effective at least for breast cancer diagnosis.

CK19 was most abundantly found in the PEG5k-precipitated EVs, but comparable amounts were also detected in the PEG20k-precipitated and ExoQuick-precipitated EVs. The harvest using PEG5k for the breast cancer cells still seemed to be effective in this case, but the reason for the detection of large amounts of CK19 in the PEG20k-precipitated and ExoQuick-precipitated EVs cannot be readily explained. The expression level of CK19 in exosomes, which mainly constitute the small-sized EV class, might be relatively low. However, the amounts of the precipitates obtained using PEG20k or ExoQuick were about four to five times larger than that obtained with PEG5k, which could explain the comparable amount of CK19 detected in the PEG20k-precipitated and ExoQuick-precipitated EVs. These observations suggested that the behaviors of EpCAM and CK19 are different in small-sized EVs.

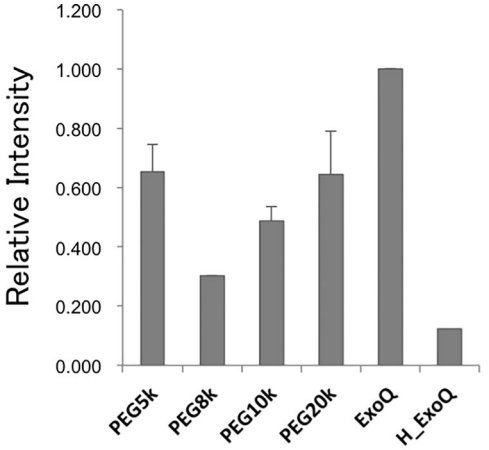

Fig. 4 Bar chart representations of ELISA experiments using CK19 as an antigen ($n = 3$). The heights of the bars were normalized to the intensities of the ExoQuick-precipitated samples from MCF-7 (ExoQ). The value from the same experiment, using the ExoQuick precipitate from HCT116, is indicated for reference (H_ExoQ) (*top*). The list of p values calculated for all combinations of PEGs (PEG5k, PEG8k, PEG10k, and PEG20k), ExoQuick, and ExoQuick-precipitated HCT116 sample (H_ExoQ), in which significantly low p values ($p < 0.05$) are highlighted in *bold* (*bottom*)

p values

miR16	PEG5k	PEG8k	PEG10k	PEG20k	ExoQ	H_ExoQ
PEG5k	-	0.1206	0.3536	0.9679	0.1208	0.1633
PEG8k	-	-	0.1164	0.1913	**2.13E-05**	0.2422
PEG10k	-	-	-	0.2744	**0.0426**	0.0646
PEG20k	-	-	-	-	0.1827	**0.0415**
ExoQ	-	-	-	-	-	0.0518

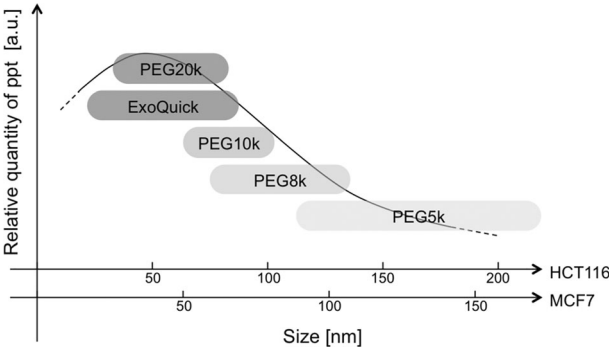

Fig. 5 Schematic diagram indicating the approximate size ranges (*horizontal*) obtained from the dynamic light scattering analyses and the roughly estimated quantities (*vertical*) of the particles precipitated by each reagent (PEG5k, PEG8k, PEG10k, PEG20k, and ExoQuick) summarized in the "Results" section. The size ranges overlapped with each other, but the ranges for PEG20k and ExoQuick did not overlap with the range of PEG5k

PEG is one of the most useful protein precipitation agents. Relatively low molecular weight PEGs (<MW 5000) are often utilized for the preferential hydration of proteins, in order to stabilize protein molecules under experimental conditions [28, 29], whereas higher molecular weight PEGs are efficient precipitating reagents for both macromolecules and lipidic vesicles, by virtue of their excluded volume effects [22]. In this study, the effect of PEG5k at the experimental concentration seemed to be insufficient for the precipitation of the small-sized EV class mainly including exosomes (40–140 nm), and thus, the sizes of the resultant precipitates predominantly ranged from 100 nm and larger. In contrast, the precipitating effect of PEG20k appeared to be fully sufficient to isolate the small-sized EV class, resulting in the highest amount of the small-sized EVs, as shown in the case of precipitating macromolecules [22, 30]. As a result, the selected PEG molecular weight ranges and their concentrations used in this study might be suitable for the size differentiation of EVs.

Conclusion

The one-step size-selective separation of EVs, including exosomes and microvesicles, utilizing various PEGs revealed that the tumor-specific miRNA and proteins were similarly distributed among the several size-sorted particle classes of the originating EVs. The size-dependent analyses of EVs in body fluid may be applicable to effective screening for tumor diagnosis.

Acknowledgments The authors are grateful to Drs. T. Sakamoto and T. Takakura at Hitachi, Ltd. for helpful discussions and Ms. I. Makino and Ms. M. Shoji at Hitachi, Ltd. for experimental assistance.

Authors' Contributions CM and HN optimized and performed the size-selective separation of particles and performed the light scattering measurement experiments. CM performed all ELISA experiments and quantitative real-time PCR experiments. TY provided the starting materials and protocols for ELISA experiments and helped to write the manuscript. CM and HN prepared the figures and wrote the manuscript. All authors commented on the manuscript and approved the final version.

Compliance with Ethical Standards

Competing Interests The authors declare that they have no competing interests.

References

1. Raposo, G., & Stoorvogel, W. (2013). Extracellular vesicles: exosomes, microvesicles, and friends. *Journal of Cell Biology, 200*, 373–383.
2. Vlassov, A. V., Magdaleno, S., Setterquist, R., & Conrad, R. (2012). Exosomes: current knowledge of their composition, biological functions, and diagnostic and therapeutic potentials. *Biochimica et Biophysica Acta, 1820*, 940–948.
3. Trams, E. G., Lauter, C. J., Salem Jr., N., & Heine, U. (1981). Exfoliation of membrane ecto-enzymes in the form of micro-vesicles. *Biochimica et Biophysica Acta, 645*, 63–70.
4. Pan, B. T., Teng, K., & Wu, C. (1985). Electron microscopic evidence for externalization of the transferrin receptor in vesicular form in sheep reticulocytes. *Journal of Cell Biology, 101*, 942–948.
5. Harding, C., Hauser, J., & Stahl, P. (1984). Endocytosis and intracellular processing of transferrin and colloidal gold-transferrin in rat reticulocytes: demonstration of a pathway for receptor shedding. *European Journal of Cell Biology, 35*, 256–263.
6. Valadi, H., Ekström, K., Bossios, A., Sjöstrand, M., Lee, J. J., & Lötvall, J. O. (2007). Exosome-mediated transfer of mRNAs and microRNAs is a novel mechanism of genetic exchange between cells. *Nature Cell Biology, 9*, 654–659.
7. Kharaziha, P., Ceder, S., Li, Q., & Panaretakis, T. (2012). Tumor cell-derived exosomes: a message in a bottle. *Biochimica et Biophysica Acta, 1826*, 103–111.
8. Hannafon, B. N., & Ding, W. Q. (2013). Intercellular communication by exosome-derived microRNAs in cancer. *International Journal of Molecular Science, 14*, 14240–14269.
9. Catto, J. Q., Miah, S., Owen, H. C., Bryant, H., Myers, K., Dudziec, E., Larre, S., Milo, A. L., & Hamdy, F. C. (2009). Distinct micro RNA alterations characterize high- and low-grade bladder cancer. *Cancer Research, 69*, 8472–8481.
10. Bartel, D. P. (2009). MicroRNAs: target recognition and regulatory functions. *Cell, 136*, 215–233.
11. Kosaka, N., Iguchi, H., Yoshioka, Y., Takeshita, F., Matsuki, Y., & Ochiya, T. (2010). Secretory mechanisms and intercellular transfer of microRNAs in living cells. *Journal of Biological Chemistry, 285*, 17442–17452.
12. Umezu, T., Ohyashiki, K., Kuroda, M., & Ohyashiki, J. H. (2013). Leukemia cell to endothelial cell communication via exosomal miRNAs. *Oncogene, 32*, 2747–2755.
13. Alvarez-Erviti, L., Seow, Y., Yin, H., Betts, C., Lakhal, S., & Wood, M. J. (2011). Delivery of siRNA to the mouse brain by systemic injection of targeted exosomes. *Nature Biotechnology, 29*, 341–345.
14. Ohno, S., Takahashi, M., Sudo, K., Ueda, S., Ishikawa, A., Matsuyama, N., Fujita, K., Mizutani, T., Ohgi, T., Ochiya, T., Gotoh, N., & Kuroda, M. (2013). Systemically injected exosomes targeted to EGFR deliver antitumor micro RNA to breast cancer cells. *Molecular Therapy, 21*, 185–191.
15. Raposo, G., Nijman, H. W., Stoorvogel, W., Liejendekker, R., Harding, C. V., Melief, C. J., & Geuze, H. J. (1996). B lymphocytes secrete antigen-presenting vesicles. *Journal of Experimental Medicine, 183*, 1161–1172.
16. Escola, J. M., Kleijmeer, M. J., Stoorvogel, W., Griffith, J. M., Yoshie, O., & Geuze, H. J. (1998). Selective enrichment of tetraspan proteins on the internal vesicles of multivesicular endosomes and on exosomes secreted by human B-lymphocytes. *Journal of Biological Chemistry, 273*, 20121–20127.
17. Wubbolts, R., Leckie, R. S., Veenhuizen, P. T., Schwarzmann, G., Möbius, W., Hoernschemeyer, J., Slot, J. W., Geuze, H. J., & Stoorvogel, W. (2003). Proteomic and biochemical analyses of human B cell-derived exosomes, potential implications for their function and multivesicular body formation. *Journal of Biological Chemistry, 278*, 10963–10972.
18. Polson, A., Potgieter, G. H., Largier, J. F., Mears, G. E. F., & Joubert, F. J. (1964). The fractionation of protein mixtures by linear polymers of high molecular weight. *Biochimica et Biophysica Acta, 82*, 463–475.
19. Juckes, I. R. (1971). Fractionation of proteins and viruses with polyethylene glycol. *Biochimica et Biophysica Acta, 229*, 535–546.
20. Rider, M. A., Hurwitz, S. N., & Meckes Jr., D. G. (2016). ExtraPEG: a polyethylene glycol-based method for enrichment of extracellular vesicles. *Scientific Reports, 6*, 23978.
21. McPherson, A. (1985). Use of polyethylene glycol in the crystallization of macromolecules. *Methods in Enzymology, 114*, 120–125.
22. Atha, D. H., & Ingham, K. C. (1981). Mechanism of precipitation of proteins by polyethylene glycols. *Journal of Biological Chemistry, 256*, 12108–12117.
23. Fouz, N., Amid, A., & Hashim, Y. Z. H. (2014). Gene expression analysis in MCF-7 breast cancer cells treated with recombinant bromelain. *Applied Biochemistry and Biotechnology, 173*, 1618–1639.
24. Nakata, B., Takashima, T., Ogawa, Y., Ishikawa, T., & Hirakawa, K. (2004). Serum CYFRA 21-1 (cytokeratin-19 fragments) is a useful tumour marker for detecting disease relapse and assessing treatment efficacy in breast cancer. *British Journal of Cancer, 91*, 873–878.

25. Jiang, S., Zhang, H. W., Lu, M. H., He, X. H., Li, Y., Gu, H., Liu, M. F., & Wang, E. D. (2010). MicroRNA-155 functions as an OncomiR in breast cancer by targeting the suppressor of cytokine signaling 1 gene. *Cancer Research, 70*, 3119–3127.
26. Corcoran, C., Friel, A. M., Duffy, M. J., Crown, J., & O'Driscoll, L. (2011). Intracellular and extracellular microRNAs in breast cancer. *Clinical Chemistry, 57*, 18–32.
27. Taylor, D. D., & Gercel-Taylor, C. (2008). MicroRNA signatures of tumor-derived exosomes as diagnostic biomarkers of ovarian cancer. *Gynecologic Oncology, 110*, 13–21.
28. Arakawa, T., & Timasheff, S. N. (1985). Mechanism of polyethylene glycol interaction with proteins. *Biochemistry, 24*, 6756–6762.
29. Bhat, R., & Timasheff, S. N. (1992). Steric exclusion is the principal source of the preferential hydration of proteins in the presence of polyethylene glycols. *Protein Science, 1*, 1133–1143.
30. Zimmerman, S. B., & Trach, S. O. (1991). Estimation of macromolecule concentrations and excluded volume effects for the cytoplasm of *Escherichia coli*. *Journal of Molecular Biology, 222*, 599–620.